Computational Models for the Multifield Analysis of Laminated Shells and related Best Theory Diagrams

E. Carrera & M. Petrolo
MUL^2 Group, Department of Mechanical and Aerospace Engineering
Politecnico di Torino, Italy

ABSTRACT: This paper presents plate and shell models for multifield problems and proposes methodologies to refine structural models according to given accuracy and computational cost requirements. In multifield problems for multilayered structures, refined models are necessary to deal with many non-classical effects due, for instance, to the presence of large variations of properties among layers. In such research scenario, the Carrera Unified Formulation (CUF) is a well-established framework. Via the CUF, the 3D structural problem is reduced to a 2D or 1D one. In other words, the 3D unknown variables become 2D or 1D, and expansion functions along the thickness or the cross-section of the structure define the order of the model, or computational cost, and its accuracy. CUF models proved to be able to detect 3D-like accuracies in multifield structural problems with very low computational costs. In the CUF framework, the axiomatic-asymptotic method (AAM) has been recently proposed by the authors to investigate the influence of each unknown variable on the solution of a given problem. And, via the AAM, Best Theory Diagrams (BTD) have been obtained in which the minimum number of terms of a refined model for a given accuracy can be read. The BTD generates guidelines to develop and evaluate structural models. In other words, via the BTD, a trade-off between accuracy and computational cost can be made. In this paper, mechanical, thermal and electrical fields are considered and BTDs are presented for various problems.

1 INTRODUCTION

Many engineering structures require multifield analyses for their proper design. For instance, thermal and mechanical loads and interaction thereof are important for space vehicles, and turbine blades. Piezoelectric and mechanical loads are fundamental in smart structures. The accurate structural analysis of such structures requires refined structural models to capture non-classical effects. In particular, the present paper presents plate and shell models for multifield analysis and a technique to build best models for given problems.

The refinement process of a plate or shell model, referred to as 2D models, is aimed at the improvement of the accuracy of classical models, such as the Kirchoff-Love (Kirchhoff 1850, Love 1927) and Reissner-Mindlin theory (Reissner 1945, Mindlin 1951). Examples of refined 2D models are those by Vlasov (1957), Hildebrand, Reissner, & Thomas (1938), and the Zig-Zag model of Lekhnitskii (1968). In the case of multilayered structures, models are usually developed according to two approaches, the Equivalent Single Layer (ESL) and the Layer Wise (LW) schemes. According to the ESL scheme, the number of the unknowns are not affected by the number of layers, while, in the LW scheme, each layer of the plate has its displacement unknowns, and, therefore, the number of unknowns of the model is related to the number of layers of the plate (Reddy 1997).

A review of methodologies for thermoelasticity can be found in (Hetnarski & Eslami 2009). 2D structural models for thermoelasticity have been developed over the last decades for isotropic, anisotropic and heterogeneous structures (Tauchert 1991, Noor & Burton 1992, Murakami 1993, Argyris & Tenek 1997). Particular attention was paid to predictor-corrector procedures, the effect of the temperature-dependence of the material properties, and the sensitivity of the thermomechanical response to variations in the material parameters, and non-linear effects.

Electromechanical effects must be considered in piezoelectric structures. Such systems are being increasingly used as sensors, actuators and energy harvesters for various applications, including control and health-monitoring. 2D, reference ESL structural models for piezoelectric structures can be found in (Tiersten 1969, Mindlin 1972, Yang & Yu 1993). On the other hand, an LW model for the electric potential coupled with an ESL displacement field can be found

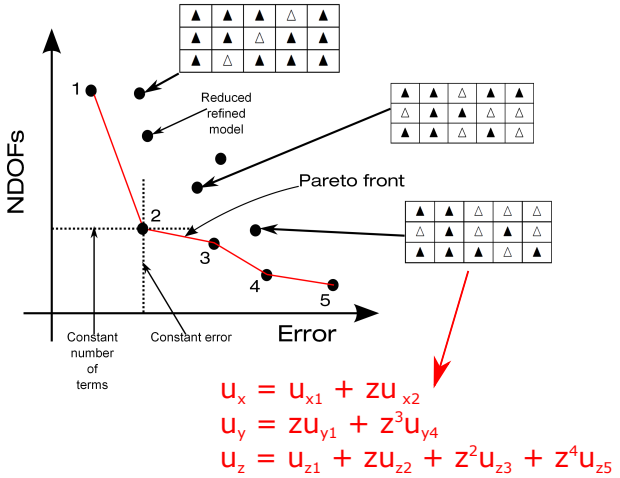

Figure 1: The Best Theory Diagram.

in (Mitchell & Reddy 1995).

This work makes use of the Carrera Unified Formulation (CUF) to build refined 2D models (Carrera et al. 2014). The CUF introduced a systematic approach to develop any-order structural model via a few fundamental nuclei whose formal expressions do not depend on the order of the model nor on the type of expansions adopted to describe the unknown variable fields (Carrera 2003). In particular, ESL, LW and mixed variational formulations can be implemented (Carrera et al. 2011). The CUF has been extensively used for multifield analyses over the last years. Reference works are those by Carrera (2002) and Ballhause et al. (2005).

In the CUF framework, the axiomatic-asymptotic method (AAM) has been recently proposed by the authors to investigate the influence of each unknown variable on the solution of a given problem (Carrera & Petrolo 2010, Carrera & Petrolo 2011). In the AAM, a starting model is used with a full expansion of variables. Then, the influence of each variable, or groups of variables, is evaluated by deactivating it. Only those variables exhibiting an influence are retained and reduced models are built in which the number of unknown variables are less or equal to the starting, full model. The method can be iterated to evaluate the influence of characteristic parameter such as thickness or orthotropic ratios, similarly to an asymptotic method. Recently, the AAM has been applied to multifield problems (Cinefra et al. 2015, Carrera et al. 2015). The systematic use of CUF and AAM has then led to the definition of Best Theory Diagrams (BTD) in which, for a given accuracy and problem, the minimum number of required unknown variables can be read, as shown in Fig. 1. The BTD can be seen as a tool to evaluate the accuracy and the computational efficiency of any given structural model against the best available. The BTD for multifield problems has been recently presented in (Cinefra et al. 2017).

This paper is organized as follows: the CUF is introduced in Section 2, governing equation in Section 3, the AAM and BTD in Section 4. The results are presented in Section 5 and Conclusions in Section 6.

2 CARRERA UNIFIED FORMULATION

In the CUF, the displacement field for a 2D model can be written as

$$\mathbf{u}(x,y,z) = F_\tau(z)\mathbf{u}_\tau(x,y) \qquad \tau = 1,\ldots,N+1 \quad (1)$$

where the Einstein notation is assumed on the index τ. $\mathbf{u}$ is the displacement vector $(u_x\ u_y\ u_z)$. F_τ are the so-called thickness expansion functions and $\mathbf{u}_\tau$ is the vector of the generalized unknown displacements. In ESL, F_τ are defined on the overall thickness of the plate, while, in LW, for each k-layer. For ESL, F_τ can be Mc-Laurin expansions of z, defined as $F_\tau = z^{\tau-1}$. In the following, the ESL models are indicated as EDN, in which N is the expansion order. For instance, the ED3 displacement field is

$$\begin{aligned} u_x &= u_{x_1} + z\,u_{x_2} + z^2\,u_{x_3} + z^3\,u_{x_4} \\ u_y &= u_{y_1} + z\,u_{y_2} + z^2\,u_{y_3} + z^3\,u_{y_4} \\ u_z &= u_{z_1} + z\,u_{z_2} + z^2\,u_{z_3} + z^3\,u_{z_4} \end{aligned} \quad (2)$$

LW models can be obtained via Legendre polynomial expansions in each layer,

$$\begin{aligned} &\mathbf{u}^k = F_t \cdot \mathbf{u}_t^k + F_b \cdot \mathbf{u}_b^k + F_r \cdot \mathbf{u}_r^k = F_\tau \mathbf{u}_\tau^k \\ &\tau = t,b,r \quad r = 2,3,\ldots,N \qquad k = 1,2,\ldots,N_L \end{aligned} \quad (3)$$

where N_L is the number of the layers. Subscripts t and b correspond to the top and bottom surfaces of the layer. Functions F_τ depend on the coordinate ζ_k, $-1 \leq \zeta_k \leq 1$. F_τ are linear combinations of the Legendre polynomials,

$$\begin{aligned} F_t &= \tfrac{P_0+P_1}{2} \qquad F_b = \tfrac{P_0-P_1}{2} \\ F_r &= P_r - P_{r-2} \qquad r = 2,3,\ldots,N \end{aligned} \quad (4)$$

In the following, the LW models are denoted by the acronym as LDN, where N is the expansion order. For instance, LD3 is

$$\begin{aligned} u_x^k &= F_t\,u_{xt}^k + F_2\,u_{x2}^k + F_3\,u_{x3}^k + F_b\,u_{xb}^k \\ u_y^k &= F_t\,u_{yt}^k + F_2\,u_{y2}^k + F_3\,u_{y3}^k + F_b\,u_{yb}^k \\ u_z^k &= F_t\,u_{zt}^k + F_2\,u_{z2}^k + F_3\,u_{z3}^k + F_b\,u_{zb}^k \end{aligned} \quad (5)$$

ESL and LW descriptions can be used for multifield variables, such as temperature or potential. For instance, the LW description of the temperature distribution is

$$\begin{aligned} &\theta^k(x,y,z) = F_t \cdot \theta_t^k(x,y) + F_r \cdot \theta_r^k(x,y) + \\ &+F_b \cdot \theta_b^k(x,y) = F_\tau \theta_\tau^k(x,y) \end{aligned} \quad (6)$$

where θ_τ^k are

$$\theta_\tau^k = \bar{\theta}_\tau^k - \theta_e \quad (7)$$

$\overline{\theta}_\tau^k$ is the effective temperature distribution. The temperature distribution can be defined by solving the conduction equation for a given temperature distribution over the lateral, top and bottom surfaces. The approach proposed in Eq.(6) offers the possibility to impose the continuity of the temperature distribution along the thickness direction. In (Carrera 2002), further details on the temperature distribution evaluation can be found. On the other hand, assumed profiles can be used, such as the linear one,

$$\theta_z = \theta_z^0 \frac{2\,z}{h} + \overline{\theta}_0 \tag{8}$$

where h is the total thickness of the plate and the parameters θ_z^0 and $\overline{\theta}_0$ are the imposed top and bottom values.
In an electro-mechanical problem, the potential distribution can be defined as

$$\begin{array}{l} \Phi^k = F_t\Phi_t^k + F_r\Phi_r^k + F_b\Phi_b^k = F_\tau\Phi_\tau^k \\ \tau = t,r,b \;\; r = 2,3,\ldots,N \end{array} \tag{9}$$

3 CONSTITUTIVE AND GOVERNING EQUATIONS

In this section, a brief overview of some of the constitutive equations adopted for multifield problems are given. For a more comprehensive overview, books from the authors can be referred to (Carrera et al. 2014, Carrera et al. 2011). Linear strain-displacement relations are assumed and strain components are grouped into in-plane (p) and out-of-plane (n), components,

$$\boldsymbol{\epsilon}_p^k = \left[\epsilon_{xx}^k \;\; \epsilon_{yy}^k \;\; \epsilon_{xy}^k\right]^T \qquad \boldsymbol{\epsilon}_n^k = \left[\epsilon_{xz}^k \;\; \epsilon_{yz}^k \;\; \epsilon_{zz}^k\right]^T \tag{10}$$

For the pure mechanical case, stress components for a generic layer k can be obtained by means of the Hooke law,

$$\boldsymbol{\sigma}^k = \mathbf{C}^k\boldsymbol{\epsilon}^k \tag{11}$$

The virtual variation of the strain energy is

$$\begin{array}{l} \delta\, L_{int}^k = \sum_{k=1}^{N_L}\int_{V_k}\left(\delta\boldsymbol{\epsilon}_p^k\cdot\boldsymbol{\sigma}_p^k + \delta\boldsymbol{\epsilon}_n^k\cdot\boldsymbol{\sigma}_n^k\right)\,dV_k = \\ \sum_{k=1}^{N_L}\int_{\Omega_k}\int_{A_k}\left(\delta\boldsymbol{\epsilon}_p^k\cdot\boldsymbol{\sigma}_p^k + \delta\boldsymbol{\epsilon}_n^k\cdot\boldsymbol{\sigma}_n^k\right)\,d\Omega_k\,dz_k \end{array} \tag{12}$$

In the case of the uncoupled thermo-mechanical analysis, thermal stresses are given by

$$\begin{array}{l} \boldsymbol{\sigma}_{pT}^k = \mathbf{C}_{pp}^k\cdot\boldsymbol{\epsilon}_{pT}^k + \mathbf{C}_{pn}^k\cdot\boldsymbol{\epsilon}_{nT}^k \\ \boldsymbol{\sigma}_{nT}^k = \mathbf{C}_{pn}^k\cdot\boldsymbol{\epsilon}_{pT}^k + \mathbf{C}_{nn}^k\cdot\boldsymbol{\epsilon}_{nT}^k \end{array} \tag{13}$$

Via the thermal expansion coefficient vector α,

$$\begin{array}{l} \boldsymbol{\epsilon}_{pT}^k = \left\{\alpha_1^k,\;\alpha_2^k,\;0\right\}\theta^k(x,y,z) = \boldsymbol{\alpha}_p^k\theta^k \\ \boldsymbol{\epsilon}_{nT}^k = \left\{0,\quad 0,\quad \alpha_3^k\right\}\theta^k(x,y,z) = \boldsymbol{\alpha}_n^k\theta^k \end{array} \tag{14}$$

where $\theta^k(x,y,z)$ is the relative temperature distribution in a generic k layer referred to a reference temperature θ_e. The virtual variation of the strain energy is

$$\sum_{k=1}^{N_l}\int_{\Omega_k}\int_{A_k}\left(\delta\boldsymbol{\epsilon}_p^{k^T}\boldsymbol{\sigma}_p^k + \delta\boldsymbol{\epsilon}_n^{k^T}\boldsymbol{\sigma}_n^k\right)\,dz_k\,d\Omega_k \tag{15}$$

where stresses $\boldsymbol{\sigma}_p$ and $\boldsymbol{\sigma}_n$ are considered as the sum of the mechanical (H) and thermal (T) contributions,

$$\begin{array}{l} \boldsymbol{\sigma}_p = \boldsymbol{\sigma}_{pH}^k - \boldsymbol{\sigma}_{pT}^k \\ \boldsymbol{\sigma}_n = \boldsymbol{\sigma}_{nH}^k - \boldsymbol{\sigma}_{nT}^k \end{array} \tag{16}$$

The constitutive equations for piezoelectric materials are

$$\begin{array}{l} \boldsymbol{\sigma}^k = \mathbf{C}^k\boldsymbol{\epsilon}^k - \mathbf{e}^{k^T}\mathbf{E}^k \\ \\ \tilde{\mathbf{D}}^k = \mathbf{e}^k\boldsymbol{\epsilon}^k + \boldsymbol{\varepsilon}^k\mathbf{E}^k \end{array} \tag{17}$$

where $\tilde{\mathbf{D}}^k$ is the dielectric displacement and $\mathbf{E}^k$ is the electric field. $\mathbf{e}^k$ is the matrix of the piezoelectric constants,

$$\mathbf{e}^k = \begin{bmatrix} 0 & 0 & 0 & e_{14}^k & e_{15}^k & 0 \\ 0 & 0 & 0 & e_{24}^k & e_{25}^k & 0 \\ e_{31}^k & e_{32}^k & e_{36}^k & 0 & 0 & e_{33}^k \end{bmatrix} \tag{18}$$

and $\boldsymbol{\varepsilon}^k$ is the matrix of the permittivity coefficients of the k-layer,

$$\boldsymbol{\varepsilon}^k = \begin{bmatrix} \varepsilon_{11}^k & \varepsilon_{12}^k & 0 \\ \varepsilon_{21}^k & \varepsilon_{22}^k & 0 \\ 0 & 0 & \varepsilon_{33}^k \end{bmatrix} \tag{19}$$

Introducing the usual in-plane (p) and out-of-plane (n) grouping,

$$\begin{array}{l} \boldsymbol{\sigma}_p^k = \mathbf{C}_{pp}\boldsymbol{\epsilon}_{pp}^k + \mathbf{C}_{pn}\boldsymbol{\epsilon}_{pn}^k - \mathbf{e}_p^{k^T}\mathbf{E}^k \\ \\ \boldsymbol{\sigma}_n^k = \mathbf{C}_{pn}^T\boldsymbol{\epsilon}_{pp}^k + \mathbf{C}_{nn}\boldsymbol{\epsilon}_{pn}^k - \mathbf{e}_n^{k^T}\mathbf{E}^k \\ \\ \tilde{\mathbf{D}}^k = \mathbf{e}_p^k\boldsymbol{\epsilon}_p^k + \mathbf{e}_n^k\boldsymbol{\epsilon}_n^k + \boldsymbol{\varepsilon}^k\mathbf{E}^k \end{array} \tag{20}$$

The electric field $\mathbf{E}^k$ can be derived from the Maxwell equations,

$$\mathbf{E}^k = \mathbf{D}_e\Phi^k \tag{21}$$

where Φ^k is the electric potential. The virtual variation of the strain energy is

$$\sum_{k=1}^{N_L}\int_{V_k}\left(\delta\boldsymbol{\epsilon}_p^{k^T}\boldsymbol{\sigma}_p^k + \delta\boldsymbol{\epsilon}_n^{k^T}\boldsymbol{\sigma}_n^k - \delta\mathbf{E}^{k^T}\;\tilde{\mathbf{D}}^k\right)\,dV_k \tag{22}$$

The governing equations are obtained substituting the geometrical relations, the constitutive equations and the variable assumptions via CUF in the variational statements. The derivation is herein omitted for the sake of brevity; details can be found in the already mentioned CUF works and books.
The governing equations in the case of pure-mechanical analysis can be written as

$$\delta \mathbf{u}_s^{k^T} : \mathbf{K}_d^{k\tau s} \mathbf{u}_\tau^k = \mathbf{P}_{d\tau}^\tau \tag{23}$$

and the boundary conditions on the edge Γ^k as

$$\delta \mathbf{u}_s^{k^T} : \mathbf{u}_k^\tau = \overline{\mathbf{u}}_k^\tau \quad \text{or} \quad \mathbf{\Pi}_d^{k\tau s} \mathbf{u}_\tau^k = \mathbf{\Pi}_d^{k\tau s} \overline{\mathbf{u}}_\tau^k \tag{24}$$

where $\mathbf{P}_{d\tau}^\tau$ is the external load. The fundamental nucleus of the stiffness matrix, $\mathbf{K}_d^{\tau s}$, is assembled through the indexes τ and s, which consider the order of the expansion in z for the displacements. $\mathbf{\Pi}_d^{k\tau s}$ is the fundamental nucleus of the boundary conditions deriving from the integration by parts of the PVD. The explicit form of the fundamental nuclei can be found in (Carrera 2003).
The governing equations for the thermo-mechanical problem, that are

$$\delta \mathbf{u}_s^{k^T} : \mathbf{K}_{uu}^{k\tau s} \mathbf{u}_\tau^k = -\mathbf{K}_{u\theta}^{k\tau s} \theta + \mathbf{p}_{us}^k \tag{25}$$

with the related boundary conditions are

$$\delta \mathbf{u}_s^{k^T} : \mathbf{u}_k^\tau = \overline{\mathbf{u}}_k^\tau \quad \text{or} \quad \mathbf{\Pi}_{uu}^{k\tau s} \mathbf{u}_\tau^k = \mathbf{\Pi}_{uu}^{k\tau s} \overline{\mathbf{u}}_\tau^k \tag{26}$$

The temperature is considered as an external load and it is assigned. The definition of the fundamental nuclei $\mathbf{K}_{uu}^{k\tau s}$, $\mathbf{K}_{u\theta}^{k\tau s}$ and $\mathbf{\Pi}_{uu}^{k\tau s}$ can be found in (Carrera & Brischetto 2010).
The governing equations for the electro-mechanical problem are:

$$\begin{aligned} \delta \mathbf{u}_k^s : &\quad \mathbf{K}_{uu}^{k\tau s} \mathbf{u}_\tau^k + \mathbf{K}_{ue}^{k\tau s} \mathbf{\Phi}_\tau^k = \mathbf{p}_{ms}^k \\ \delta \mathbf{\Phi}_k^s : &\quad \mathbf{K}_{eu}^{k\tau s} \mathbf{u}_\tau^k + \mathbf{K}_{ee}^{k\tau s} \mathbf{\Phi}_\tau^k = \mathbf{p}_{es}^k \end{aligned} \tag{27}$$

with the boundary conditions,

$$\begin{aligned} &\delta \mathbf{u}_k^s : \ \mathbf{u}_k^\tau = \overline{\mathbf{u}}_k^\tau \quad \text{or} \\ &\quad \mathbf{\Pi}_{uu}^{k\tau s} \mathbf{u}_\tau^k + \mathbf{\Pi}_{ue}^{k\tau s} \mathbf{\Phi}_\tau^k = \mathbf{\Pi}_{uu}^{k\tau s} \overline{\mathbf{u}}_\tau^k + \mathbf{\Pi}_{ue}^{k\tau s} \overline{\mathbf{\Phi}}_\tau^k \\ &\delta \mathbf{\Phi}_k^s : \ \mathbf{\Phi}_k^\tau = \overline{\mathbf{\Phi}}_k^\tau \quad \text{or} \\ &\quad \mathbf{\Pi}_{eu}^{k\tau s} \mathbf{u}_\tau^k + \mathbf{\Pi}_{ee}^{k\tau s} \mathbf{\Phi}_\tau^k = \mathbf{\Pi}_{eu}^{k\tau s} \overline{\mathbf{u}}_\tau^k + \mathbf{\Pi}_{ee}^{k\tau s} \overline{\mathbf{\Phi}}_\tau^k \end{aligned}$$

The definition of the fundamental nuclei $\mathbf{K}_{uu}^{k\tau s}$, $\mathbf{K}_{ue}^{k\tau s}$, $\mathbf{K}_{eu}^{k\tau s}$, $\mathbf{K}_{ee}^{k\tau s}$, $\mathbf{\Pi}_{uu}^{k\tau s}$, $\mathbf{\Pi}_{ue}^{k\tau s}$, $\mathbf{\Pi}_{eu}^{k\tau s}$ and $\mathbf{\Pi}_{ee}^{k\tau s}$ can be found in (Ballhause et al. 2005).
In the CUF, the adoption of the fundamental nucleus to assemble the problem matrices allows us to set the order and the type of the expansion as an input of the analysis. In other words, the theory of structure to be used is an input of the analysis.

Table 1: ED4 model with u_{y_3} inactive.

z^0	z^1	z^2	z^3	z^4
▲	▲	▲	▲	▲
▲	▲	△	▲	▲
▲	▲	▲	▲	▲

4 THE AXIOMATIC/ASYMPTOTIC METHOD AND BEST THEORY DIAGRAMS

In the CUF framework, the axiomatic/asymptotic method (AAM) has been recently developed to evaluate the influence of an unknown variable on a given structural problem as we vary the problem characteristics, e.g. thickness, orthotropic ratio, stacking sequence, etc.. Also, the AAM leads to the definition of reduced models with a lower computational costs than full models but with the same accuracy (Carrera & Petrolo 2010, Carrera & Petrolo 2011). A typical AAM analysis consists of the following steps:

1. Parameters, such as the geometry, BC, loadings, materials and layer layouts, are fixed.
2. A starting theory is fixed (axiomatic part). That is, the displacement field is defined; usually a theory which provides 3D-like solutions is chosen and a reference solution is defined.
3. The CUF is used to generate the governing equations for the theories considered.
4. The effectiveness of each term of the adopted expansion is evaluated by measuring the error due to its deactivation.
5. The most suitable structural model for a given structural problem is then obtained discarding the non-effective displacement variables.

A graphical notation is introduced to show the results. It consists of a table with three lines, and columns equal to the number of the variables used in the expansion. For example, if an ED4 model is considered with u_{y_3} deactivated, the displacement field is

$$\begin{aligned} u_x = &\ u_{x_1} + &z\, u_{x_2} + &\ z^2\, u_{x_3} + &z^3\, u_{x_4} + &\ z^4\, u_{x_5} \\ u_y = &\ u_{y_1} + &z\, u_{y_2} + &\ + &z^3\, u_{y_4} + &\ z^4\, u_{y_5} \\ u_z = &\ u_{z_1} + &z\, u_{z_2} + &\ z^2\, u_{z_3} + &z^3\, u_{z_4} + &\ z^4\, u_{z_5} \end{aligned} \tag{28}$$

Such a displacement field is depicted by Table 1. The use of the AAM can be extended to all the possible combinations of active/inactive variables of a given, starting theory. Each reduced model can be related to the number of the active terms and its error computed on a reference solution as reported in Fig. 1. The error values are reported on the abscissa, and the number of active terms is reported on the ordinate. Each

black dot represents a reduced refined model and its position on the Cartesian plane is defined considering its error and the number of the active terms. Also, the representation of the active/non-active terms is reported for some reduced models. Among all the models, it is possible to note that some of them present the lowest error for a given number of active terms. These models are labeled as 1, 2, 3, 4, 5, and they represent a Pareto front for the considered problems. The Pareto front is defined in this work as the Best Theory Diagram. This curve can be constructed for several problems, for example considering several type of materials, geometries and boundary conditions. Moreover, the information reported in a BTD makes it possible to evaluate the minimum number of terms, N_{min}, that have to be used to achieve the desired accuracy.
The BTD can be obtained via genetic algorithms in which each structural theory is considered as an individual. The genes are the terms of the expansion, and each gene can be active or not active as in Fig. 2. Each individual is, therefore, described by the number

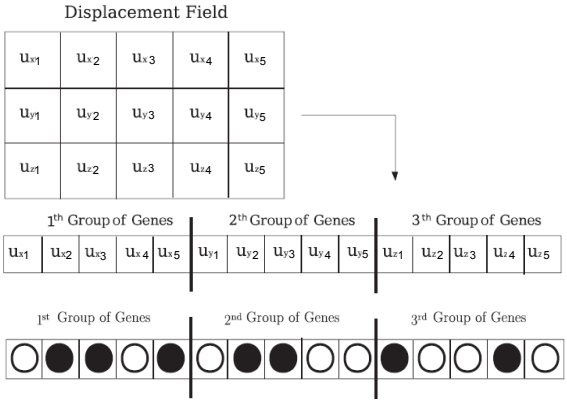

Figure 2: Generalized variables as genes in a genetic algorithm.

of active terms and its error computed on a reference solution. Through these two parameters, it is possible to apply the dominance rule in order to evaluate the individuals fitness. For each individual copies are created according to its dominance and then, some mutations are applied to vary the set of new individuals. The purpose of this analysis is to find the individuals which belong to the Pareto front, that is the subset of individuals which are dominated by no other individuals.

5 RESULTS

First, a simply-supported multilayered plate is considered under a transverse pressure distribution, a temperature distribution and an electric potential distribution, separately. For the mechanical case, the pressure distribution is

$$p_z = p_z^0 \sin\left(\frac{m\,\pi}{a}\,x\right) \sin\left(\frac{n\,\pi}{b}\,y\right) \tag{29}$$

where m and n are equal to 1, the pressure distribution is applied to the top surface of the plate, and $a = b = 1$. For the thermal case, temperature distribution defined as in

$$\theta_\tau^k = \hat{\theta}_\tau^k \sin\left(\frac{m\pi x_k}{a_k}\right) \sin\left(\frac{n\pi y_k}{b_k}\right) \tag{30}$$

and Eq. (8), with (t_{top}, t_{bot}) equal to 1 and -1, respectively. For the piezoelectric case, two different configurations were considered, the sensor and actuator configurations. In the sensor case, a transverse pressure is applied to the top surface of the plate and the potential distribution is evaluated. The potential at the top and bottom is set to zero. In the actuator case, a potential distribution is applied to the plate, and the value of the potential is set to 1 V at the top and to 0 V at the bottom. In the sensor case, the pressure is assumed as in Eq.(29), while, in the actuator case, the potential distribution is assumed as

$$\Phi = \overline{\Phi} \sin\left(\frac{m\,\pi}{a}\,x\right) \sin\left(\frac{n\,\pi}{b}\,y\right) \tag{31}$$

where $m = n = 1$ and $\overline{\Phi}$ is set equal to 1. The material properties for the mechanical and thermal cases are $E_L/E_T = 25$, $G_{LT}/E_T = G_{TT}/E_T = 0.5$, $G_{Lz}/E_T = 0.2$, $\nu = 0.25$ and $\alpha_L/\alpha_T = 1125$, where E is the Young's modulus, G the shear modulus, ν the Poisson's ratio and α the coefficient of thermal expansion. L and T are the directions parallel and transverse to the composite fibers, respectively. For the piezoelectric case, the material properties of the laminated layers are: $E_1 = 132.38 \times 10^9$ Pa, $E_2 = E_3 = 10.756 \times 10^9$ Pa, $G_{12} = G_{13} = 5.6537 \times 10^9$ Pa, $G_{23} = 3.606 \times 10^9$ Pa, $\nu_{12} = \nu_{13} = 0.24$, $\nu_{23} = 0.49$, $\varepsilon_{11} = 3.098966 \times 10^{-11}$ C/Vm, $\varepsilon_{22} = \varepsilon_{33} = 2.6562563 \times 10^{-11}$ C/Vm. The thickness for each of these layers is equal to $h = 0.4 \cdot h_{\text{TOT}}$. The piezoelectric layers are made of PZT-4 and their properties are $E_1 = E_2 = 81.3 \times 10^9$ Pa, $E_3 = 64.5 \times 10^9$ Pa, $\nu_{12} = 0.329$, $\nu_{13} = \nu_{23} = 0.432$, $G_{44} = G_{55} = 25.6 \times 10^9$ Pa, $G_{66} = 30.6 \times 10^9$ Pa, $e_{31} = e_{32} = -5.20$ C/m^2, $e_{33} = 15.08$ C/m^2, $e_{24} = e_{15} = 12.72$ C/m^2, $\varepsilon_{11}/\varepsilon_0 = \varepsilon_{22}/\varepsilon_0 = 1475$, $\varepsilon_{33}/\varepsilon_0 = 1300$ ($\varepsilon_0 = 8.854 \times 10^{-12}$ C/Vm). The thickness of these layers is equal to $h = 0.1 \cdot h_{\text{TOT}}$. The BTDs reported in this work are based on the solution computed using the LD4 model. In fact, the LD4 proved to be in excellent agreement with the elastic solutions (Carrera 2003, Carrera 2002, Ballhause et al. 2005).
The ESL approach is considered, and the BTDs for the ED4 model are given in Fig.s 3 and 4 for the thin and thick geometry, respectively. The results suggest that reduced refined models for the piezoelectric case have a higher computational cost than the reduced models for the mechanical and thermal case, since the variables of the electric potential are retained. Models located on the BTD for both the thermal and mechanical cases have the same accuracy when a thin plate is considered, while the BTDs for the piezoelectric

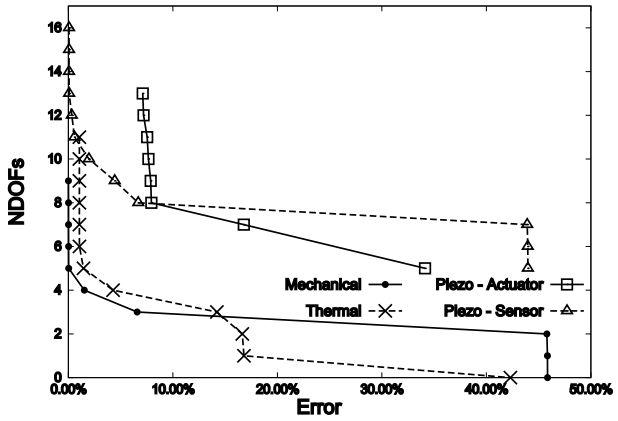

Figure 3: BTDs for $a/h = 100$.

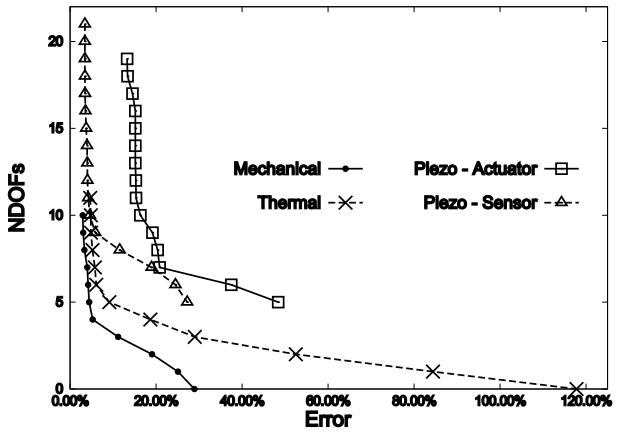

Figure 4: BTDs for $a/h = 4$.

case present a significant difference between the sensor and actuator configuration. Since the reference solution is obtained with an LD4 model, the minimum errors are larger than zero. In fact, the LD4 offers a better accuracy than ED4.
A composite shell is then considered under a pure mechanical load, see Eq. 29. The material properties are $E_L/E_T = 25$, $\nu = 0.25$, $G_{LT}/E_T = G_{TT}/E_T = 0.5$, $G_{Lz}/E_T = 0.2$ and the dimensions of the shell are $a = 4\,R_\beta$ and $b = 2\,\pi\,R_\beta$. A $0°/90°$ stacking sequence was considered. Figure 5 shows the BTD for stress and displacement components. Significant differences in the BTD for different outputs are observable. Table 2 shows some of the BTD models. In this case, the FSDT is a BTD.

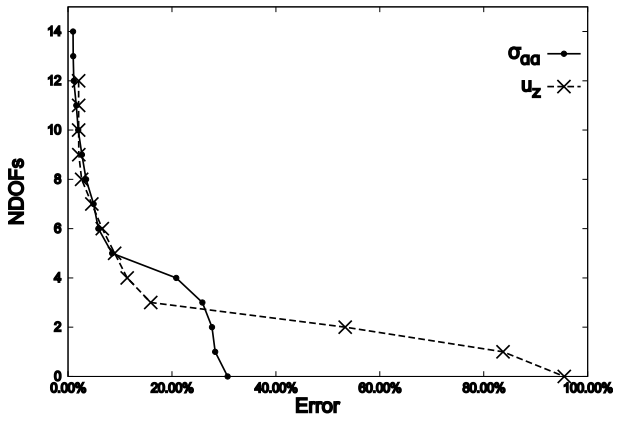

Figure 5: BTD for the asymmetric composite shells, $R_\beta/h = 4$.

Table 2: BTDs for the asymmetric composite shell, $\sigma_{\alpha\alpha}$.

$R_\beta/h = 100$				
$M_e/M = 9/15$				
▲	▲	△	△	△
▲	▲	▲	▲	△
▲	▲	▲	△	△
Error	$2.6671\,\%$			
$M_e/M = 5/15$				
▲	▲	△	△	△
▲	▲	△	△	△
▲	△	△	△	△
Error	$8.4968\,\%$			

6 CONCLUSIONS

This paper has presented some of the latest advances in the framework of the Carrera Unified Formulation (CUF). In particular, multifield problems for multilayered plates and shells have been addressed. The CUF is an established formulation to develop refined structural models via expansion functions. The order and the type of the expansions are free parameters of the analysis. In particular, Equivalent Single Layer (ESL) and Layer-Wise (LW) approaches can be handled straightforwardly.
In this work, a brief overview of the Axiomatic/Asymptotic Method (AAM) has been given. The AAM has been recently developed in the CUF framework and has two main capabilities,

- A starting structural model is set, and the influence of each unknown variable on a given structural problem is quantified as the problem characteristics vary (e.g. thickness, orthotropic ratio, stacking sequence, etc.). In other words, starting from an axiomatic approach, asymptotic-like results can be obtained.

- By retrieving only those terms that influence the solution, reduced models as accurate as the full models but computationally more efficient are built.

The systematic use of the AAM has led to the introduction of the Best Theory Diagram (BTD). A 'best theory' is the one that, for a given number of unknown variables, provides the best accuracy or, for a given accuracy, the one with the minimum number of unknown variables. In the BTD, all the best structural models can be read. The BTD can be considered as the Pareto Front of an optimization problem and provides guidelines to develop structural models. In fact, The BTD provides the boundary of the trade-off between accuracy and computational costs. In other words, accuracy cannot be increased and computational cost lowered better than the BTD.
The results show that the combined use of CUF and AAM provides insights related to the decision making in structural model choices and developments. In particular, the reduced models greatly increase the computational efficiency in the LW case. Also, the use of

genetic algorithms to obtain the BTD is a powerful strategy to obtain structural guidelines for any problem.

REFERENCES

Argyris, J. & L. Tenek (1997). Recent advances in computational thermostructural analysis of composite plates and shells with strong nonlinearities. *Applied Mechanics Reviews 50*(5), 285–306.

Ballhause, D., M. D'Ottavio, B. Kroplin, & E. Carrera (2005). A unified formulation to assess multilayered theories for piezoelectric plates. *Computer & Structures 83*, 1217–1235.

Carrera, E. (2002). Temperature profile influence on layered plates response considering classical and advanced theories. *AIAA Journal 40*(9), 1885–1896.

Carrera, E. (2003). Theories and finite elements for multilayered plates and shells: A unified compact formulation with numerical assessment and benchmarking. *Archives of Computational Methods in Engineering 10*(3), 215–296.

Carrera, E. & S. Brischetto (2010). Coupled thermo-mechanical analysis of one-layered and multilayered plates. *Composite Structures 92*(1-2).

Carrera, E., S. Brischetto, & P. Nali (2011). *Plates and Shells for Smart Structures: Classical and Advanced Theories for Modeling and Analysis*. John Wiley & Sons.

Carrera, E., M. Cinefra, A. Lamberti, & A. Zenkour (2015). Axiomatic/asymptotic evaluation of refined plate models for thermomechanical analysis. *Journal of Thermal Stress 38*, 165–187. doi: 10.1080/01495739.2014.976141.

Carrera, E., M. Cinefra, M. Petrolo, & E. Zappino (2014). *Finite Element Analysis of Structures through Unified Formulation*. John Wiley & Sons.

Carrera, E. & M. Petrolo (2010). Guidelines and recommendation to contruct theories for metallic and composite plates. *AIAA Journal 48*(12), 2852–2866. doi: 10.2514/1.J050316.

Carrera, E. & M. Petrolo (2011). On the effectiveness of higher-order terms in refined beam theories. *Journal of Applied Mechanics 78*. doi: 10.1115/1.4002207.

Cinefra, M., E. Carrera, A. Lamberti, & M. Petrolo (2017). Best theory diagrams for multilayered plates considering multifield analysis.

Cinefra, M., A. Lamberti, A. Zenkour, & E. Carrera (2015). Axiomatic/asymptotic technique applied to refined theories for piezoelectric plates. *Mechanics of Advanced Materials and Structures 22*(1-2), 107–124. doi: 10.1080/15376494.2014.908043.

Hetnarski, R. B. & M. R. Eslami (2009). *Thermal Stresses - Advanced Theory and Applications*. Springer.

Hildebrand, F. B., E. Reissner, & G. B. Thomas (1938). Notes in the foundations of the theory of small displacement of orthotropic shells. Technical report, NASA.

Kirchhoff, G. (1850). Uber das gleichgewicht und die bewegung einer elastischen scheibe. *Journal fur reins und angewandte Mathematik 40*, 51–88.

Lekhnitskii, G. S. (1968). *Anisotropic Plates*. Gordon and Breach Science Publishers.

Love, A. E. H. (1927). *The Mathematical Theory of Elasticity*. Cambridge University Press.

Mindlin, R. (1972). High frequency vibrations of piezoelectric crystal plates. *International Journal of Solids and Structures 8*, 895–906.

Mindlin, R. D. (1951). Influence of rotatory inertia and shear in flexural motions of isotropic elastic plates. *Journal of Applied Mechanics 18*, 1031–1036.

Mitchell, J. & J. N. Reddy (1995). A refined hybrid plate theory for composite laminates with piezoelectric laminae. *International Journal of Solids and Structures 32*(16), 2345–2367.

Murakami, H. (1993). Assessment of plate theories for treating the thermomechanical response of layered plates. *Composites Engineering 3*(2), 137–149.

Noor, A. K. & W. S. Burton (1992). Computational models for high-temperature multilayered composite plates and shells. *Applied Mechanics Reviews 12*(10), 419–446.

Reddy, J. N. (1997). *Mechanics of Laminated Plates, Theory and Analysis*. CRC Press.

Reissner, E. (1945). The effect of transverse shear deformation on the bending of elastic plates. *Journal of Applied Mechanics 12*, 69–76.

Tauchert, T. R. (1991). Thermally induced flexure, buckling, and vibration of plates. *Applied Mechanics Reviews 44*(8), 347–360.

Tiersten, H. F. (1969). *Linear Piezoelectric Plate Vibrations*. Plenum Press.

Vlasov, B. F. (1957). On the equations of bending of plates. *Doklady Akademii Nauk Azerbaidzhanskoi SSR 3*, 955–979.

Yang, J. & J. Yu (1993). Equations for a laminated piezoelectric plate. *Archives of Mechanics 45*, 653–664.